

Seasonal variability of surface and column carbon monoxide over megacity Paris, high altitude Jungfraujoch and Southern Hemispheric Wollongong stations

Yao Té¹, Pascal Jeseck¹, Bruno Franco², Emmanuel Mahieu², Nicholas Jones³,
Clare Paton-Walsh³, David W. T. Griffith³, Rebecca R. Buchholz⁴,
Juliette Hadji-Lazaro⁵, Daniel Hurtmans⁶, and Christof Janssen¹

¹LERMA-IPSL, Sorbonne Universités, UPMC Univ Paris 06, CNRS, Observatoire de Paris, PSL Research University, F-75005, Paris, France

²Institut d'Astrophysique et de Géophysique, Université de Liège, B-4000 Liège, Belgique

³Center for Atmospheric Chemistry, Faculty of Science, Medicine & Health, University of Wollongong NSW 2522 Australia

⁴Atmospheric Chemistry Observations & Modelling Laboratory, National Center for Atmospheric Research, Boulder, CO, USA

⁵Sorbonne Universités, UPMC Univ. Paris 06, Univ. Versailles St-Quentin, CNRS/INSU, UMR 8190, LATMOS-IPSL, Paris, France

⁶Spectroscopie de l'Atmosphère, Service de Chimie Quantique et Photophysique, Université Libre de Bruxelles, Brussels, Belgium

Correspondence to: Yao Té (yao-veng.te@upmc.fr)

Abstract. The paper studies the seasonal variation of surface and column CO at three different sites (Paris, Jungfraujoch and Wollongong), with an emphasis on establishing a link between the CO vertical distribution and the nature of CO emission sources. We find the first evidence of a time-lag between surface and free tropospheric CO seasonal cycles in the Northern Hemisphere. The CO seasonal variability obtained from the total columns and from the free tropospheric partial columns shows a maximum around March-April and a minimum around September-October in the Northern Hemisphere (Paris and Jungfraujoch). In the Southern Hemisphere (Wollongong) this seasonal variability is shifted by about 6 months. Satellite observations by the IASI-MetOp and MOPITT instruments confirm this seasonality. Ground-based FTIR (Fourier Transform InfraRed) measurements provide useful complementary information due to good sensitivity in the boundary layer. In situ surface measurements of CO volume mixing ratios in Paris and at Jungfraujoch reveal a time-lag of the near-surface seasonal variability of about 2 months with respect to the total column variability at the same sites. The chemical transport model GEOS-Chem is employed to interpret our observations. GEOS-Chem sensitivity runs allow identification of the emission sources influencing the seasonal cycle of CO. In Paris and at Jungfraujoch, the surface seasonality is mainly driven by anthropogenic emissions, while the total column seasonality is also controlled by air masses transported from dis-

tant sources. In Wollongong, where the CO seasonality is mainly affected by biomass burning, no time shift is observed between surface measurements and total column data.

1 Introduction

20 Atmospheric carbon monoxide (CO) is an important trace gas. It has direct and indirect impact on air quality due to its toxicity and its effect on the atmospheric oxidizing capacity. The major sources of CO are fuel and energy-related industries, heating, motor vehicle transport, biomass burning, and the secondary oxidation of methane and of volatile organic compounds (VOCs such as isoprene and terpene), which are emitted by plants. Due to the fast reaction



CO is the major sink for the main atmospheric oxidation agent, the hydroxyl radical OH (Weinstock, 1969; Bakwin et al., 1994). A global increase of atmospheric CO thus leads to a decrease in global OH, which in turn augments the concentration of other, potentially harmful atmospheric trace gases (Logan et al., 1981; Thompson et al., 1990; Thompson, 1992) or potent greenhouse gases sensitive
30 to oxidation such as methane, which contributes about one-third to the total sources of CO (Duncan et al., 2007; Holloway et al., 2000). Before 1980, there were only few measurements, which showed an increase of CO in the Northern Hemisphere (Khalil and Rasmussen, 1988; Zander et al., 1989), probably related to an increase of anthropogenic emissions (Novelli et al., 1998). From end of 1980 until 1997, CO has decreased (Khalil and Rasmussen, 1994; Novelli et al., 1994). Since then, few
35 large episodic increases of CO, associated with unusual large forest fires, have been observed in the Northern Hemisphere (Novelli et al., 2003; Yurganov et al., 2004, 2005). Bekki et al. (1994) have observed a negative trend in CO, that was attributed to the Mount Pinatubo eruption in June 1991. In the Southern Hemisphere no significant trends were observed (Brunke et al., 1990; Novelli et al., 2003). Global observations of CO were initiated through the start of the flask sampling program of
40 the NOAA¹ Earth System Research Laboratory, Global Monitoring Division (Novelli et al., 1994, 1998, 2003). In parallel, CO total column observations were performed at several locations (Mahieu et al., 1997; Zhao et al., 1997; Rinsland et al., 1998, 1999, 2000).

This paper characterizes the CO seasonal variability at three ground-based FTIR sites: Paris megacity, high-altitude Jungfraujoch and Southern Hemisphere Wollongong. These sites have been
45 selected for their representativeness of different environments (remote vs. moderate and high pollution sites, Northern vs. Southern Hemisphere) and meteorological conditions:

- Megacity of Paris (France): A high-resolution Fourier transform spectrometer from Bruker Optics (FTS-Paris) has been installed in 2006 on the campus of “Université Pierre et Marie

¹National Oceanic and Atmospheric Administration

Curie” in the centre of the French capital Paris (48°50’47”N, 2°21’21”E, 60 m asl). Since then,
50 the instrument has been continuously operated by LERMA².

– Jungfraujoch (Switzerland): The International Scientific Station of the Jungfraujoch (ISSJ) is
located in the Swiss Alps (46°33’N, 7°58’48”E, 3580 m asl). Two FTIR instruments have been
used at that site, a homemade FTIR from 1984 to 2008 and a commercial Bruker IFS 120 HR
from the early 1990 to present. University of Liège (Belgium) is responsible for the operation
55 of the infrared instruments at Jungfraujoch.

– Wollongong (Australia): The station is located in the Southern Hemisphere at Wollongong
University (34°24’22”S, 150°52’44”E, 30 m asl). The instrument, which is also a commer-
cial high-resolution Fourier transform spectrometer (Bruker IFS 125HR), is operated by the
University of Wollongong and provides data since 1996.

60 All three ground-based FTIR spectrometers are part of NDACC (Network for the Detection of Atmo-
spheric Composition Change) and/or TCCON (Total Carbon Column Observing Network) networks
and have monitored the concentration of CO for several years. Paris is the first ground-based FTIR
station located in a European megacity which provides rare hot spot measurements of atmospheric
species related to anthropogenic activities. The remote high-altitude Jungfraujoch station provides
65 one of the longest observational time series for a variety of atmospheric gases. Wollongong is a sta-
tion exposed to moderate levels of pollution and is located at the East coast of Australia and about
80 km from the South of Sydney. Here, we present NDACC analysis data on the seasonal variations
of CO and compare the results from the different sites. The ground-based remote sensing measure-
ments are compared with results from the satellite instruments IASI-MetOp (Infrared Atmospheric
70 Sounding Interferometer (Tournier et al., 2002)) and MOPITT (Measurements Of Pollution In The
Troposphere (Drummond and Mand, 1996)). With respect to satellite measurements, ground-based
FTIR instruments are more sensitive to the boundary layer and can therefore provide complementary
data which we compare with in situ measurements at the surface. Due to specific conditions at the
ground, the surface and the total column seasonalities might differ from each other. Using GEOS-
75 Chem modeling (Goddard Earth Observing System - chemical transport model (CTM), Bey et al.
(2001)) simulations, we investigate the impact of local sources on the lower partial column and its
variability as compared to the total column.

The paper is structured as follows. In section 2, the remote sensing instruments and measurements
are described. Section 3 presents the in situ analyser measurements and the GEOS-Chem model
80 simulation data. Section 4 shows the CO total column variability obtained from the remote sensing
data and the one from the surface in situ measurements. Both results are compared to the GEOS-
Chem model simulations, which is also used to identify emission sources at each site.

²Laboratoire d’études du Rayonnement et de la Matière en Astrophysique et Atmosphères

2 Remote sensing instruments and measurements

2.1 Instrumentation and measurements at Paris, France

85 The FTS-Paris is a Michelson interferometer from Bruker Optics. Table 1 lists technical details on
the ground-based FTIR instruments as well as the configuration used for the measurements. Solar
absorption spectra are acquired by coupling the FTS to a sun-tracker installed on the roof terrace.
The solar disk is tracked with an accuracy of less than 1 arcmin. Using appropriate band pass filters
allows the optimisation of the signal-to-noise ratio when focussing on specific target gases. The Paris
90 instrument is part of TCCON (TCCON-Paris station). But for the present CO study, the FTS-Paris
uses optical elements corresponding to a typical NDACC configuration. More instrumental details
and different measurement configurations are given elsewhere (Té et al., 2010, 2012).

Only clear sky spectra were analysed. Available solar spectra cover the time period from May
2009 to the end of 2013, with only very few spectra (about 400 spectra during 19 measurement
95 days) for the period between 2009 and 2010. Between 2011 and 2013, spectra acquisition was more
frequent and more than 4500 spectra from 117 measurement days were recorded and analysed. The
absorption lines of each atmospheric species observed in the solar spectra are used to retrieve its
abundance in the atmosphere by appropriate radiative transfer and inversion algorithms (Pougatchev
and Rinsland, 1995; Zhao et al., 1997; Hase et al., 2006). We have used the PROFFIT algorithm
100 developed by F. Hase to analyse the Paris data using the HITRAN 2008 spectral database (Rothman
et al., 2009). PROFFIT is a code especially adapted for the analysis of solar absorption spectra from
the ground and it has been widely applied and tested (Hase et al., 2004; Duchatelet et al., 2010;
Schneider et al., 2010; Té et al., 2012; Viatte et al., 2011). For the retrieval of CO, we have selected
two micro-windows. The $2110.4 - 2110.5 \text{ cm}^{-1}$ micro-window is centred around the weak $R(3)$ line
105 of ^{13}CO , which is more sensitive to CO at higher altitudes and the $2111.1 - 2112.1 \text{ cm}^{-1}$ micro-
window around the strongly saturated $P(8)$ line of ^{12}CO . The left and right wings of that line are
particularly sensitive to CO in the Planetary Boundary Layer (PBL). The retrieval uses a grid with
49 altitude levels and, on average, there are about 2.7 degrees of freedom (DOF). The uncertainties
in the CO column density and the profile stem from a variety of sources. These sources have been
110 investigated in detail by Té et al. (2012), following the procedure outlined by Rinsland et al. (2000).
According to this evaluation, the random uncertainty is around 2.5%. Concerning the systematic
uncertainties of about 3 to 6.8% (Té et al., 2012), the largest source is linked to the quality
of available spectroscopic parameters (line intensity and air-broadened half-width uncertainties in
Rothman et al. (2009)), which is similar for the three sites.

115 2.2 Instrumentation and measurements at Jungfraujoch, Switzerland

The Jungfraujoch station in Switzerland is part of NDACC and the instrumental setup is similar
to the one in Paris, cf. Table 1. A thorough description of the instrumentation is given by Zander

et al. (2008). Infrared solar spectra are recorded under clear-sky conditions and, thanks to the high altitude, the interference by water vapour is very low. The integration time is either 135, 404 or 1035 s, corresponding to 3 or 9 scans of 45 s, or 15 scans of 69 s. High resolution observations are only recorded under slowly varying geometry, i.e. for zenith angles lower than $\sim 70^\circ$.

The Jungfraujoch data set corresponds to an update of the CO time series described by Dils et al. (2011). It covers the January 2009 to December 2013 time period and includes 1733 individual spectra recorded on 539 different days. Mean signal-to-noise ratio (S/N) is 2930, with the 2nd percentile still being above 1000. The SFIT-2 (v3.91) algorithm (Rinsland et al., 1998) based on the semi-empirical implementation of the Optimal Estimation Method (OEM) of Rodgers (1990) is used, allowing retrieval of information on the vertical profile of most FTIR target gases. The standard NDACC approach for the CO retrieval is adopted, to simultaneously fitting three micro-windows spanning the 2057.7 – 2058.0, 2069.56 – 2069.76 and 2157.3 – 2159.15 cm^{-1} intervals. The line parameters correspond to the standard release of HITRAN 2004 (Rothman et al., 2005), including the August 2006 updates (e.g. Esposito et al., 2007). The a priori mixing ratio profiles for all interfering molecules (main telluric absorptions by N_2O , O_3 , H_2O and CO_2) correspond to a mean of the 1975-2020 version 4 WACCM model (the Whole Atmosphere Community Climate Model; <https://www2.cesm.ucar.edu/working-groups/wawg>) simulation performed for the Jungfraujoch. The CO a priori vertical distribution combines WACCM results above 15.5 km, ACE-FTS occultation measurements between 6.5 and 15.5 km (version 2.2, Clerbaux et al., 2008) and extrapolation of ACE-FTS data down to the station altitude, ending at 137 ppbv in the first retrieval layer (3.58 – 4.23 km). Additional retrieval settings include a S/N ratio of 150 for inversion, the a priori covariance matrix, with diagonal elements close to 30%/km in the troposphere and extra-diagonal elements computed assuming a Gaussian inter-layer correlation half-width length of 4 km. Objective evaluation of the resulting typical information content indicates that 2 independent pieces of information are available (DOF of 2.2 on average). Typical random uncertainties have been evaluated at 2 – 3% for the total columns and 5% for the 3.58 – 7.18 km partial columns.

2.3 Instrumentation and measurements at Wollongong, Australia

The Wollongong instrument is part of both NDACC and TCCON. The instrument setup is similar to the Paris and Jungfraujoch spectrometers (see Table 1). Using the NDACC configuration, CO total and partial column data are produced using 3 micro-windows in the 4.6 μm band of CO (Zeng et al., 2015).

The analysis of the Wollongong NDACC data is very similar to the method described in section 2.2 for the Jungfraujoch data. The algorithm used was SFIT4 v9.4.4 (<https://wiki.ucar.edu/display/sfit4/Infrared+Working+Group+Retrieval+Code,+SFIT>), an updated version of SFIT2 used in the Jungfraujoch analysis. SFIT4 has inherited the same forward model and inverse method but with a number of enhancements (not required in the CO analysis), and gives the same results in the CO

retrieval. For the Wollongong data, HITRAN 2008 was adopted (Rothman et al, 2009), the mean of
155 the 1980-2020 WACCM version 4 run used as the a priori CO profile (and a 4 km Gaussian interlayer
correlation), with the a priori covariance matrix set to 1 standard deviation of the WACCM profiles. A
measurement signal-to-noise ratio of 200 was assumed. This gives a mean DOF of 2.7. The version
4 WACCM profiles were also used for the a priori profiles of all actively fitted interfering gases
(O₃, H₂O, N₂O, CO₂, etc.). The error analysis used a NDACC community Python tool to estimate
160 errors assuming a solar zenith angle of 50.2°, representing the mean zenith angle for all Wollongong
spectra. The resulting CO total column random errors were calculated to be 2.2%.

2.4 Satellite instruments and measurements

The IASI Michelson interferometer (Infrared Atmospheric Sounding Interferometer, Tournier et al.
(2002); Blumstein et al. (2004)) is flying on-board the Meteorological operation (MetOp) polar Orbit
165 platform. The first platform (MetOp-A) was launched on October 19, 2006 and operational data
have been provided since October 2007. IASI operates at an altitude of around 817 km on a sun-
synchronous orbit with a 98.7° inclination to the equator. It overpasses each region twice a day.
The MetOp platform has a swath of 30 views of 50 km by 50 km comprising four off-axis pixels of
12 km diameter footprint each at nadir. A second platform (MetOp-B) was launched in September
170 2012 and the launch of the third and last platform (MetOp-C) is scheduled for October 2018. IASI
observations provide an important contribution to the monitoring of atmospheric composition over
time (Clerbaux et al., 2009).

The IASI-MetOp is a Fourier transform spectrometer with a medium spectral resolution of 0.5 cm⁻¹
and a radiometric noise of about 0.2 K at 280 K using nadir viewing and working in the thermal
175 infrared (TIR) range extending from 645 to 2760 cm⁻¹ with no gaps. The CO products (L2) are
downloaded from the ETHER database, cf. <http://www.pole-ether.fr>, for the period from January 1,
2009 to December 31, 2013. The total column data were generated from the IASI radiance spectra
in the 4.7 μm spectral range and from IASI L2 meteorological data (surface and vertical profile of
temperature, humidity vertical profile and cloud cover) (August et al., 2012), using the Fast Optimal
180 Retrievals on Layers for IASI (FORLI) code (Hurtmans et al., 2006). The CO total columns were
compared to other CO satellite data (George et al., 2009), from which a DOF value of about 2 was
provided and a relative uncertainty between 4% and 10% could be estimated. The total columns are
calculated from the ground altitude to 60 km height. For this paper, we also provide additional verti-
cal volume mixing ratio (VMR) profiles and partial columns in the PBL and in the troposphere layers
185 around Île-de-France; as well as the partial columns above 4 km height around the Jungfrauoch site.

The MOPITT instrument (Drummond and Mand, 1996; Deeter et al., 2004) is on-board the
NASA's Terra spacecraft in a sun-synchronous polar orbit at an altitude of 705 km. The satellite
was launched on December 18, 1999. MOPITT has been operational since March 2000. The instru-
ment uses the technique of gas-filter correlation radiometry based on the IR absorption bands of CO

190 to retrieve the vertical profiles of CO. The horizontal footprint of each MOPITT retrieval is 22 km by 22 km.

The MOPITT data were downloaded from the NASA website, cf. <https://eosweb.larc.nasa.gov/datapool>. We are using version 6 retrievals of CO vertical profiles and total columns, for the period from the beginning of 2009 to the end of 2013. The MOPITT retrieval history can be found at the link
195 <https://www2.acd.ucar.edu/mopitt/products>. Since version 5 of the MOPITT retrieval algorithm, TIR (4.7 μm) radiances are combined with the near IR (2.3 μm) daily radiances to improve the sensitivity to lower tropospheric CO over land. The DOF value is about 2 (Worden et al., 2010). The retrieved vertical VMR profile is reported on 10 pressure levels (at the surface and every hundred hPa between 900 and 100 hPa). The retrieved CO total columns are obtained by integrating the retrieved VMR
200 profile. In this paper, we are using the level 2 TIR/NIR products.

In order to be compared to the ground-based FTIR data, satellite data were selected when they are located in a 30 km \times 30 km square centered at the site location: 0.15° around the site latitude and 0.23° around the site longitude.

3 In situ analyser measurements and GEOS-Chem model simulation data

205 3.1 Surface in situ measurements at Paris

Continuous in situ measurements of the CO surface concentration are performed using a commercial analyser (CO11M, Environnement SA). The operating principle of the CO analyser is based on the CO infrared absorption at 4.67 μm , which is the same spectral band covered by the FTS-Paris. Ambient atmospheric air is drawn from the building rooftop into the analyser via PTFE tubing using
210 a diaphragm pump, which is limited to a gas flow of 80 litres per hour. The pumped air is analysed in a 20 cm length multi-path absorption cell with an absorption path length of 5.6 m, using a global IR source and a photoconductive PbSe detector. The CO analyser has a sensitive range between 0.1 and 200 ppmv, with an uncertainty of 50 ppbv for each individual measurement. Recorded values are time averages over 15 minutes. For the present paper, daily in situ surface CO measurements are
215 available for the whole period between beginning of 2009 and end of 2013.

3.2 Surface in situ measurements in Switzerland

Swiss in situ surface data are from the Swiss National Air Pollution Monitoring Network (NABEL), which is a network of 16 observation sites distributed throughout Switzerland in order to measure and record long-term measurement series of air pollutants. The NABEL monitoring network is operated
220 by EMPA. The monitoring stations are representative of different pollution levels. The monthly averaged data were obtained from the annual reports published by the Swiss OFEV (Office fédéral de l'Environnement, <http://www.bafu.admin.ch/publikationen/00016>). For the paper, we have focussed

on the urban sites Bern, Lausanne, Lugano and Zürich as well as the remote mountain station of Jungfrauoch.

225 3.3 Surface in situ measurements at Wollongong

Results of surface CO at Wollongong were obtained from two high-precision in situ FTIR trace gas analysers (Griffith et al., 2012). The analysers use an IR source, modulated through a Michelson interferometer with a CaF₂ beamsplitter. The modulated IR beam is passed through a dried atmospheric sample within a White cell in a 24 m folded-path and subsequently detected by thermo-
230 electrically cooled MCT (Mercury Cadmium Telluride) detector. Ambient air is measured daily over 23.5 hours, with 30 minutes reserved for calibration using constant composition air. Ambient air is flushed through an inlet line at 5 L/min and sample air is continuously drawn from this line through the instrument at 1 L/min. The Spectronus™ software (Ecotech P/L, Knoxfield, VIC, Australia) is used to automate internal valve control and stabilise parameters, such as flow, pressure and temper-
235 ature. Recorded spectra are averaged over 3 minutes. Non-linear least-squares fitting of CO occurs in two broad spectral regions (from 4.33 to 4.65 μm and from 4.46 to 4.76 μm), using the program MALT (Multiple Atmospheric Layer Transmission, Griffith (1996)). Data are reported as dry-air mole fraction, with a total relative measurement uncertainty below 1%. Wollongong CO measurements were first analysed by Buchholz et al. (2016) and are publicly available as 10 minute averages
240 via PANGAEA (doi:10.1594/PANGAEA.848263). In situ data was monthly averaged and selected to cover the period from June 2012 to May 2013.

3.4 Data from the GEOS-Chem model

The global 3-D chemical transport model GEOS-Chem (version 9-02: <http://acmg.seas.harvard.edu/geos/doc/archive/man.v9-02>) can be used to simulate global trace gas (more than 100 tracers) and
245 aerosol distributions. The model is driven by the Goddard Earth Observing System v5 (GEOS-5) assimilated meteorological fields from the NASA Global Modeling Assimilation Office (GMAO), which are at a native horizontal resolution of 0.5° × 0.667°. The GEOS-5 data describe the atmosphere from the surface up to 0.01 hPa with 72 hybrid pressure-σ levels, at a 6 h temporal frequency (3 h for surface properties and mixing depths). In this study, we use the degraded GEOS-5 meteorological fields as model input to a 2° × 2.5° horizontal resolution and 47 vertical levels, lumping
250 together levels above ~ 80 hPa. We apply here the standard full chemistry GEOS-Chem simulation, including detailed O₃ – NO_x – Volatile Organic Compound (VOC) – aerosol coupled chemistry (Bey et al. (2001); Park et al. (2004); with updates by Mao et al. (2010)).

Tropospheric CO is emitted from anthropogenic, biomass burning and biofuel burning sources, as
255 well as from the degradation of many VOCs. The emission inventory of the emissions database for Global Atmospheric Research (EDGAR; <http://edgar.jrc.ec.europa.eu>) v3.2 (Olivier and Berdowski, 2001) is the global reference for anthropogenic emissions of CO, NO_x, SO_x, and NH₃. For global

anthropogenic sources of Non-Methane VOCs (NMVOCs), GEOS-Chem uses the REanalysis of the TROpospheric chemical composition (RETRO; http://gcmd.gsfc.nasa.gov/records/GCMD_GEIA_RETRO) emission inventory (Schultz et al., 2007) for the base year 2000. However, these global inventories may be overwritten by regional emission inventories such as over Europe, where the anthropogenic emissions of CO, NO_x, SO_x, NH₃, propene, acetaldehyde, methyl ethyl ketone and higher C3 alkanes are provided by the European Monitoring and Evaluation Programme (EMEP; <http://www.ceip.at>) regional inventory for the year 2010 (Benedictow et al., 2010). All these global and regional inventories are scaled to the years of interest according to the method described by van Donkelaar et al. (2008). Anthropogenic sources of ethane and propane are derived from an offline simulation (Xiao et al., 2008). The global biomass burning emissions are provided by the Global Fire Emissions Database (GFED) v3 (van der Werf et al., 2010) and the global biogenic emissions are obtained with the Model of Emissions of Gases and Aerosols from Nature (MEGAN) v2.1 (Guenther et al., 2006)). Methane concentrations in GEOS-Chem are based on measurements from the NOAA Global Monitoring Division flask measurements.

The GEOS-Chem data set employed in the present work covers the period from January 2009 to May 2013 and is derived from a July 2005 to May 2013 simulation, for which the GEOS-5 meteorological fields are available. A 1-year run preceding this simulation was used for chemical initialization of the model. The model outputs consist of CO VMR profiles simulated at the closest pixel to each station and saved at a 3 h time step. The vertical resolution and the sensitivity of the FTIR retrievals have been taken into account for the comparisons involving GEOS-Chem results: the individual VMR profiles produced by the model have been first regridded onto the vertical layer-scheme adopted at each station, then daily averaged and finally smoothed by convolution with the FTIR averaging kernels (AVKs) according to the formalism of Rodgers and Connor (2003). The regridding method used here is a mass conservative interpolation that preserves the CO total mass simulated above the altitude of the station (the CO mass below is ignored). The AVKs employed for smoothing are seasonal averages (over March – May, June – August, September – November and December – February, respectively) derived from the individual retrievals of the 2009 – 2013 FTIR data sets. The smoothing did not change the comparison results between the model and our observations (difference smaller than 1%).

4 Seasonal variability

4.1 Remote sensing observations

Figure 1 shows the CO total columns of the three ground-based FTIR sites from 2009 to the end of 2013. The data from Paris are less numerous than from the other two sites, because measurements are not fully automated and spectral acquisitions are only launched when clear sky is expected for more than half of the daytime. Moreover, from 2009 to 2010, Paris CO spectra were recorded only during

intensive measurement campaigns, and not on a regular basis. As expected, the CO abundance is higher in the Northern Hemisphere. The CO column mean value is about 2.1×10^{18} molecules/cm² at Paris which is almost twice as high as the value at Wollongong (1.3×10^{18} molecules/cm²). The CO mean value of 1.1×10^{18} molecules/cm² at Jungfraujoch is quite low due to the site's height.

All three sites clearly display a seasonal variability of CO. For its characterisation, we have used a sine function (Eq. (1)). This is in agreement with previous studies conducted by Rinsland et al. (2000, 2001, 2007) and Zhao et al. (2002), but in comparison to Rinsland et al., we have removed the linear term, because our data sets do not show any significant trend:

$$y = y_0 + A \sin\left(\pi \frac{t - t_c}{w}\right). \quad (1)$$

Here y represents the abundance of CO (in total or partial columns or volume mixing ratio); y_0 is the mean value (offset); A and w respectively are the amplitude and the half-period of the seasonal cycle; t and t_c the date and the phase shift. Table 2 summarizes the fit results for w and A obtained at the three sites.

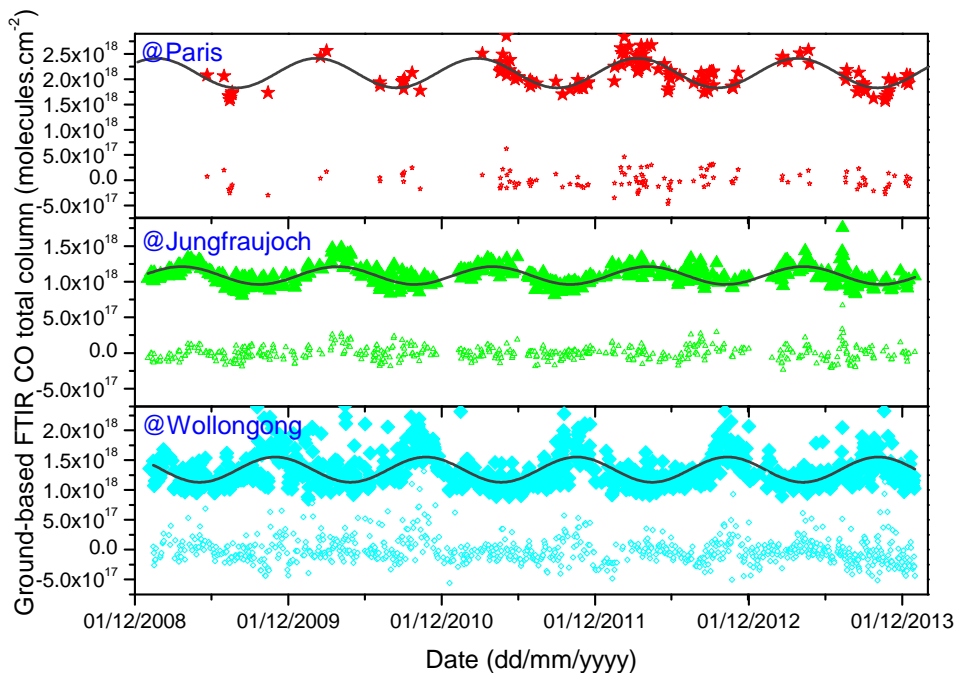


Figure 1. CO total columns retrieved by ground-based FTIR instruments at Paris (top), Jungfraujoch (middle) and Wollongong (bottom). Dark gray lines present CO seasonal variability at each station fitted with sine functions. Open symbols represent the residuals from the sine fit.

For the Northern Hemisphere (Paris and Jungfraujoch), the maximum is observed around March-April and the minimum around September-October. The average amplitude of the seasonal variability

ity is about $(13 \pm 3)\%$ of the column average and the average half-cycle is about 188 ± 4 days for both Northern hemispheric sites. For Paris, the value $w = 191 \pm 3$ days is slightly, but not significantly higher, probably due to the lack of data before 2011. This seasonal variability is also observed by Rinsland et al. (2007) at Kitt Peak, which is the US National Solar Observatory at 2.09 km altitude located in the Northern Hemisphere, by Barret et al. (2003) at the Jungfraujoch, and by Zhao et al. (2002) for Northern Japan. Our observations also agree with a recent 11 years climatology on purely tropospheric CO columns at Northern hemispheric sites (Zbinden et al., 2013), where observed maxima fall within the period from February to April. In the Southern Hemisphere, we observe an expected shift of 6 months as compared to the Northern Hemisphere, with a maximum in October and a minimum in April. The average half-period is about 178 ± 1 days. We also note that the relative amplitude of the seasonal variation is slightly higher at Wollongong (17%) than at Paris, but it remains close within error bars. Interestingly, the relative amplitude is lowest at Jungfraujoch, where the impact of local surface emissions is small.

The seasonal variability of CO is also observed by the IASI-MetOp and MOPITT instruments, cf. Fig. 2 and Table 2. One of the advantages of the satellite measurements is their spatial coverage. In general, the period and the amplitude of the seasonal variability obtained from the satellite data agree with the corresponding values from the ground-based FTIR measurements. For the Jungfraujoch station, the satellite data need to be recalculated in order to correspond to the column between the ground altitude and the top of the atmosphere (Barret et al., 2003), because the large satellite footprint not only includes the site, but also neighboring areas of lower altitude. Concerning the IASI-MetOp data, the contributions from levels below the Jungfraujoch altitude have been subtracted from the total columns. For the MOPITT data, we extracted the retrieved CO profile for Jungfraujoch and interpolated the lower pressure levels in a thinner vertical grid in order to calculate the column between the given ground altitude and the top of the atmosphere. MOPITT measurements are performed for specific ground altitudes which, however, are not made available. We have assumed a ground altitude of about 1100 m which is the mean altitude for the Bern canton,³ to which the Jungfraujoch belongs. Partial columns above 1100 m were then calculated using the interpolated CO vertical profiles and daily NCEP meteorological pressure and temperature profiles. Data from the ground-based FTIR instruments and the satellites are in good agreement. This is demonstrated in Fig. 3, where the satellite data are plotted against the ground-based measurements. The good agreement is indicated by robust fits yielding slopes of 0.98 for Paris, 0.91 for Jungfraujoch and 0.99 for Wollongong. The robust fit regression is based on a process called iteratively reweighted least squares (Street et al., 1988) and is less sensitive than ordinary least squares to large changes in small parts of the data.

GEOS-Chem model outputs are presented in Fig. 2 over the entire period from the beginning of 2009 until June 2013. The model is in good agreement with ground-based observations (R^2 between

³<https://lta.cr.usgs.gov/GTOPO30> (Global 30 Arc-Second Elevation)

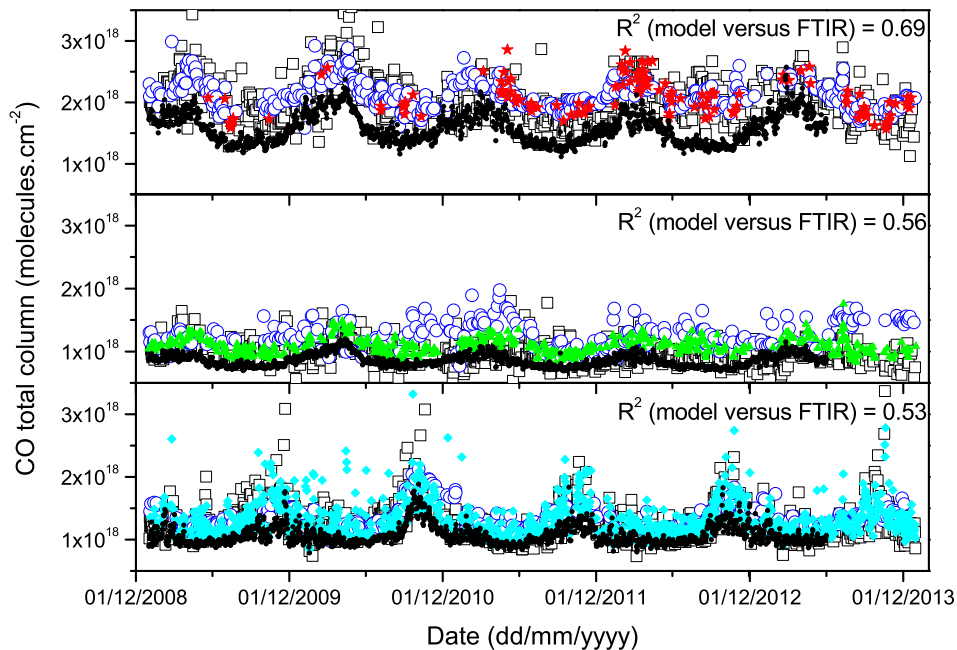


Figure 2. Time series of CO columns from satellite instruments and ground-based FTIR are given for Paris, Jungfraujoch and Wollongong (from top to bottom). IASI-MetOp and MOPITT columns are displayed as black open squares and blue open circles. Ground-based FTIR CO total columns are shown by red stars, green triangles and cyan diamonds for Paris, Jungfraujoch and Wollongong, respectively. GEOS-Chem CO total columns are indicated by full circles in black colour.

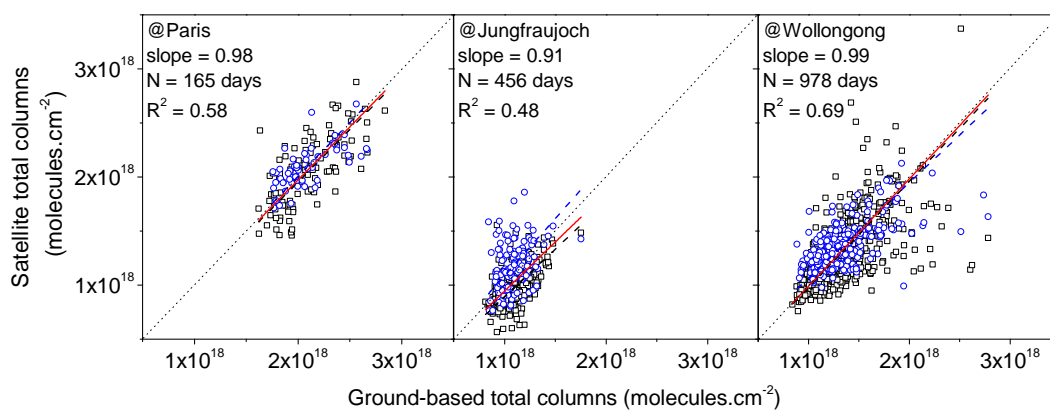


Figure 3. Correlation between satellites (IASI and MOPITT) and ground-based FTIR total columns at the three different sites, IASI data are in black squares and MOPITT data in blue circles. The dark dotted line and the blue one are the robust regression fit results for respectively IASI-MetOp and MOPITT. Slope values are obtained using both data sets (red line).

0.53 and 0.69), even if the observed total atmospheric CO abundance is underestimated at all three
345 sites: the relative deviations are commensurate: -24% for Paris, -21% for Jungfraujoch, and -20%
for Wollongong. In Duncan et al. (2007), the averaged bias between observations and GEOS-Chem
model simulations is less than $\pm 10\%$, but for some sites (Seychelles or Tae-Ahn), the bias can ex-
ceed $\pm 20\%$. Zeng et al. (2015) have observed large underestimations from models as compared to
350 the ground-based FTIR stations in the Southern Hemisphere ranging from -19.2% to -27.5% and
depending on the emission inventories implemented in the models for the Wollongong site (episodic
events unaccounted for in the emission inventories). The present deviations are also consistent with
previous inverse modeling studies (Kopacz et al., 2010; Hooghiemstra et al., 2012) and could orig-
inate from an underestimation of the emissions of CO and of its VOC precursors in the inventories
355 currently implemented in GEOS-Chem. Nonetheless, exploring this discrepancy was beyond the
scope of this paper that aims at studying the seasonal variability of CO and not at reproducing ob-
served concentrations. It has thus to be underlined that the model shows the same seasonal variability
as the measurements: GEOS-Chem simulations reproduce the Northern Hemispheric maximum in
March-April and the minimum in September-October and the model is therefore appropriate for
diagnosing the seasonal variability. Both, the period and the relative amplitude of the variability
360 are comparable to the measurement results, cf. Table 2. The lower R^2 between GEOS-Chem and
ground-based FTIR for Jungfraujoch and Wollongong as compared to Paris, are probably due to the
more complex orography at these two sites: Jungfraujoch is located in the highest Swiss Alps and the
surroundings show very large differences in altitude; Wollongong is sandwiched between the ocean
(Tasman sea) and a hilly region (Blue mountains) with a typical altitude of a few hundred meters.

365 4.2 In situ measurements of surface CO

Daily averages of the surface CO concentration during the 2009 – 2013 period at Paris are plotted in
the bottom panel of Fig. 4. Since only very few FTS-Paris data are available for the winter months
January and December, the corresponding monthly means have not been presented in Fig. 4.

The figure shows a clear seasonal variability with a maximum around January-February and a
370 minimum around July-August. The amplitude of the seasonal variation is about 30%, which is larger
than the total column variability. This shows the stronger and more direct influence of local CO
emissions due to anthropogenic activities, which are expected to be particularly high in a megac-
ity. As mentioned in Sect. 2.1, the retrieval grid (49 levels) provides a much thinner atmospheric
layering than the effective vertical resolution indicated by the averaging kernels (Rodgers, 1990).
375 The CO averaging kernels for each altitude of the a priori profile indicate a good sensitivity of the
FTS-Paris instrument to the PBL. Effectively, the left panel of the figure 5 shows that the retrieval
of CO essentially provides two independent measurement points of tropospheric CO: the first point
supplies maximal information in the altitude range between 0 and 1000 m and thus well represents
the PBL. The second one is representative of the upper troposphere, with a maximum around 8-9 km.

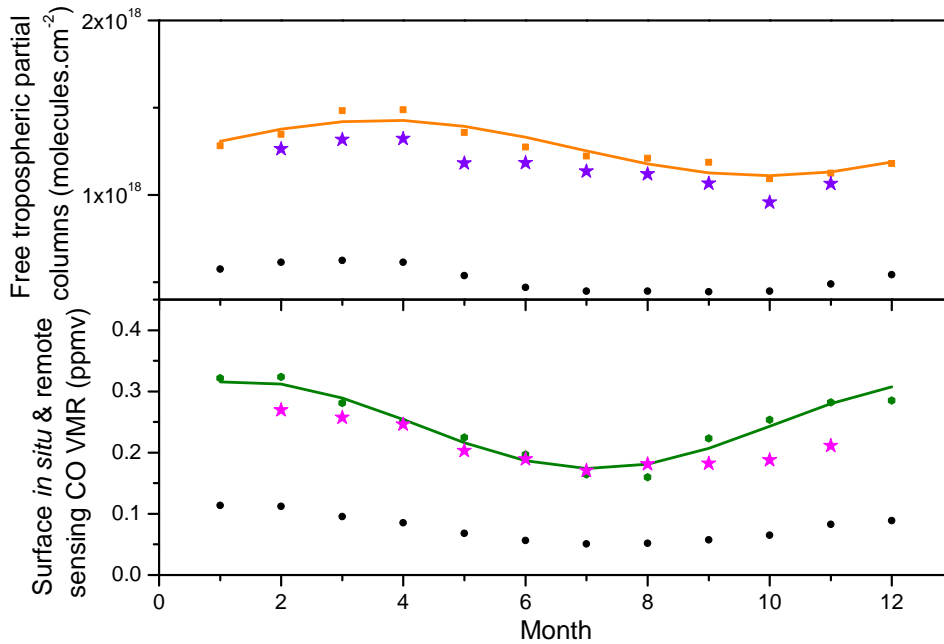


Figure 4. Free tropospheric (top) and surface (bottom) CO at Paris as monthly averages over 5 years. CO VMR in the PBL come from the in situ CO analyser (dark green hexagons) and from the FTS-Paris (magenta stars), as well as from the GEOS-Chem model (black circles). Free tropospheric CO columns were calculated between 2 and 12 km and monthly averaged over the period from 2009 to 2013. Shown are data from IASI-MetOp (orange squares), FTS-Paris (purple stars) and from GEOS-Chem modeling (black circles). A sine function fit is applied to the IASI-MetOp (orange line) and in situ CO data (dark green line).

380 The FTS-Paris data in the bottom panel of Fig. 4 represent the averaged CO VMR obtained for the altitude range between the ground (60 m asl) and the 1000 m level. These remote sensing measurements are consistent with the in situ data, even if they are much less affected by local pollution peaks. By comparing Figs. 1 and 4, we notice that the seasonal variability of the total column is shifted by about 2 months as compared to the variability at the surface. The free tropospheric columns of
 385 CO have been calculated as partial columns between 2 and about 12 km over Paris for both, IASI-MetOp and FTS-Paris. The right panel of the figure 5 shows the July 2010 monthly averaged AVKs of IASI-MetOp. These AVKs show a relatively low surface sensitivity which is more emphasised during winter (we have also checked the January 2010 monthly averaged AVKs not shown here). We thus only exploit the partial columns corresponding to the free troposphere. The seasonal variability
 390 in the free troposphere obtained by the three different kinds of data is also shifted by two months as compared to the surface seasonal variation. In addition to local surface sources, column abundances are influenced by the transport of down wind emission sources. The surface seasonal variability is

directly influenced by the local emission due to human activities: fossil fuel combustion, domestic heating, and industrial activities. In contrast, the total column seasonal variability is additionally
 395 influenced by emissions from distant sources that get transported into the upper levels of the atmosphere. The surface CO maximum in January-February corresponds to the winter season, where domestic heating is strong and where the PBL height is reduced. Additionally, oxidation by OH is lowest due to weak actinic flux. The minimum in July-August, where the PBL height is highest, not only corresponds to an increased oxidization of CO by OH, whose abundance is influenced by solar
 400 ultraviolet radiation (Bousquet et al., 2005; Rohrer and Berresheim, 2006; Duncan et al., 2007), but also to the summer vacation season during which the inhabitants of Paris usually leave the city (by more than 50%, <http://www.insee.fr>), leading to a drastic decrease of vehicle traffic. In order to check the consistency of the GEOS-Chem model, we have plotted the GEOS-Chem surface VMR in the bottom panel of the Fig. 4. The model confirms the time shift between surface and total column
 405 seasonal variability, with a maximum at the end of January-February and a minimum at the end of July-August. We once again notice an underestimation of the surface CO VMR by the GEOS-Chem model. The discrepancy of about -37% is larger than the difference of -24% between GEOS-Chem and ground-based total columns, and can probably be attributed to strong local emissions, which are not in the current emission inventories implemented in GEOS-Chem.

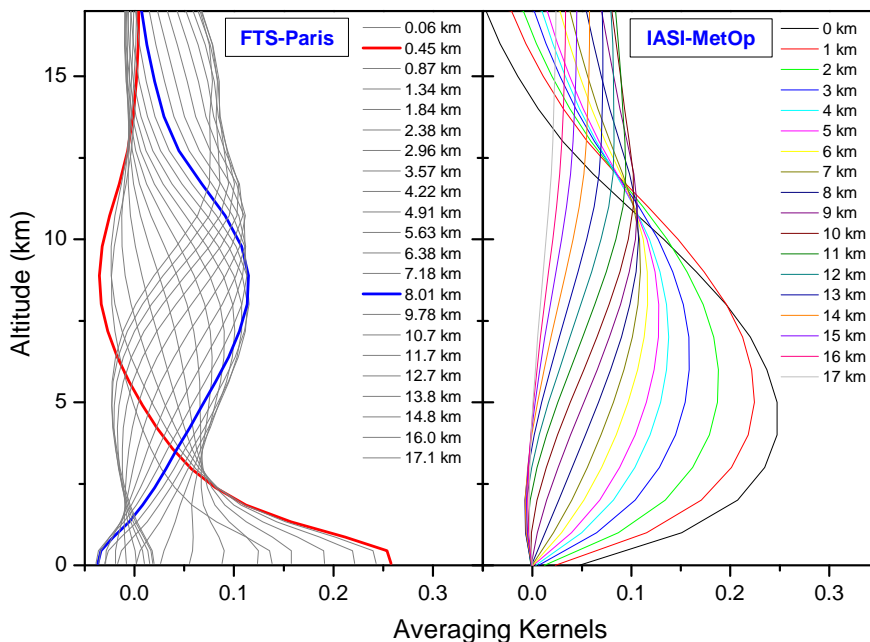


Figure 5. CO averaging kernels for each altitude of the a priori profile (from 0 to 17 km) for FTS-Paris (left panel) and IASI-MetOp (right panel).

410 There is also a temporal shift in seasonal cycles between the surface and the high altitudes in
 Switzerland, as indicated by the difference between urban and mountain sites. This is shown in
 Figure 6 that compares the four urban NABEL sites with an average altitude of 438.25 m asl to the
 in situ surface CO obtained on top of Jungfrauoch at the altitude of 3578 m asl. The low-altitude
 sites show a similar seasonal variability to the surface CO at Paris, with a maximum around January
 415 and a minimum around July. Zellweger et al. (2009) point out that the in situ observations at Swiss
 urban stations reliably represent the mixture of traffic and industrial emissions.

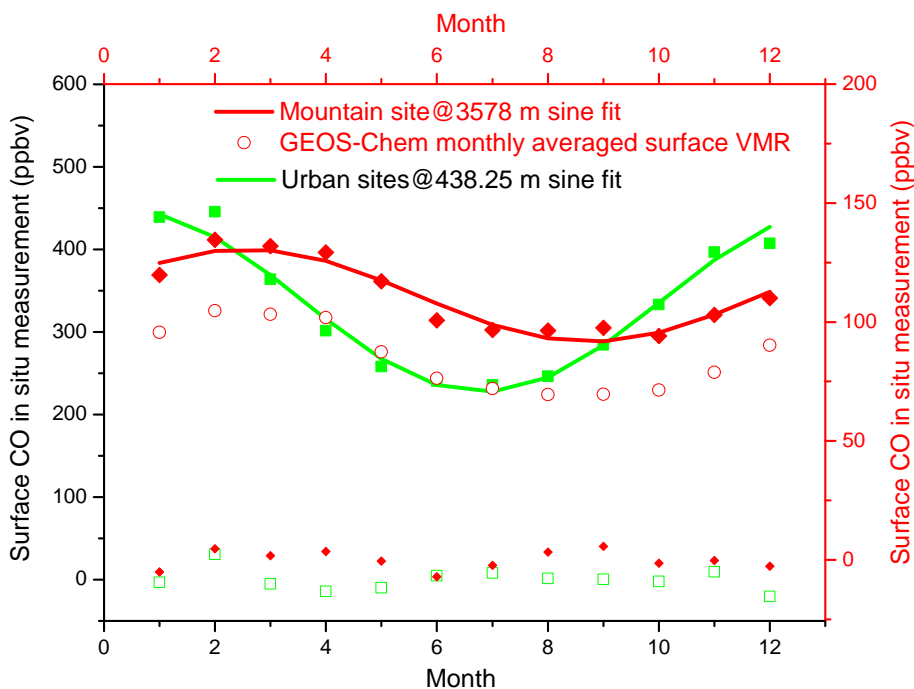


Figure 6. 5 years monthly averaged CO in situ measurements at the surface in Switzerland using Swiss NABEL data from 2009 to 2013 (green squares for the four urban sites means and red diamonds for Jungfrauoch). The sine function fit is applied on the 5 years monthly means of urban sites (green line) and of mountain site (red line). The below part shows the residuals of the fit (green open squares for urban sites and red small diamonds for Jungfrauoch). Monthly averaged CO surface VMR from GEOS-Chem model located at Jungfrauoch (red open circles).

Quite differently, in situ surface CO at Jungfrauoch shows the same seasonal variability as the whole atmosphere (characterized by the total column seasonality) being shifted by 2 months with respect to the urban sites. This is in agreement with the GEOS-Chem modeling at Jungfrauoch.
 420 Unlike the modeling for Paris where the underestimation is much stronger, the GEOS-Chem underestimates the CO surface VMR by about 23%, which is similar to the 21% difference obtained for

the total columns. This is consistent with the much lower influence from low altitude emissions and from the PBL.

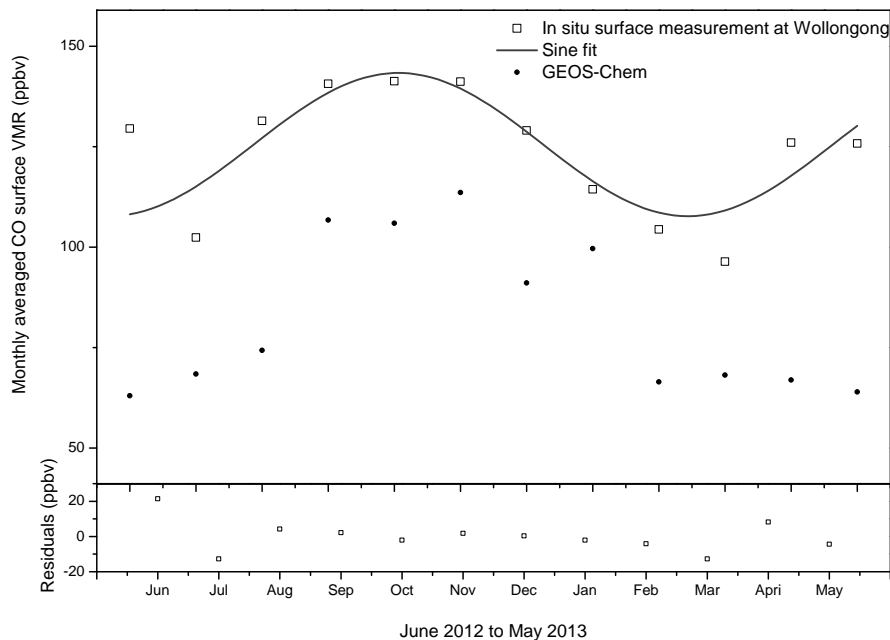


Figure 7. Monthly averaged CO surface VMR at Wollongong from in situ measurements (black open squares) and from GEOS-Chem model (black full circles) from June 2012 to May 2013. The sine function fit residuals are shown in the bottom panel.

Figure 7 shows the monthly averaged surface CO in situ measurements performed at Wollongong between June 2012 and May 2013. We observe a surface seasonality with a maximum around October and a minimum in February-March. The maximum corresponds to elevated biomass burning levels during the Southern Hemispheric spring (Edwards et al., 2006). Unlike the two Northern Hemispheric sites, there seems to be no significant time shift between the CO seasonal variabilities at the Wollongong surface level and at higher altitudes. This suggests that the Wollongong surface atmosphere is more representative of the free troposphere. The GEOS-Chem monthly averaged surface VMR shows a maximum during the austral spring and a lower level after the end of the austral summer until the austral winter. A striking increase after March 2013 is observed by the surface in situ measurements, but not by the GEOS-Chem model. This might be due to close-by local emission sources which are probably not referenced in the inventories implemented in GEOS-Chem. A longer time series of these measurements will be helpful to better understand this observation. The background seasonality of CO is mainly driven by biomass burning sources modulated by the

OH sink, (Buchholz et al., 2016). Similar to Paris, the surface CO discrepancy between model and measurement of -33% is slightly increased as compared to the value of -20% for the total columns.

4.3 Emission sources impacting the seasonality of CO columns

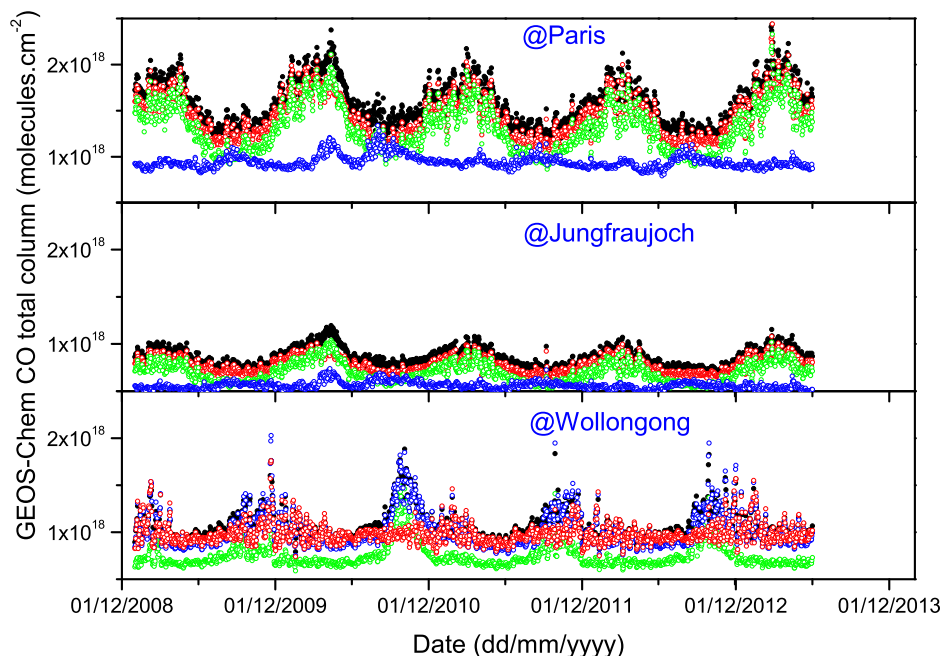


Figure 8. GEOS-Chem time series of CO total columns for Paris (top), Jungfraujoch (middle) and Wollongong (bottom). Different colors indicate standard run (black), run without biomass burning (red), run without biogenic emissions (green) and run without anthropogenic emissions (blue).

440 In order to study the influence of the different categories of CO and NMVOC emissions on the CO total column and its seasonality at the three sites, another three GEOS-Chem simulations have been run. These relied on the same setup as for the standard run (standard chemistry, horizontal resolution, time period. . .), but in each of these runs we turned off either the biogenic, the anthropogenic (incorporating the biofuel emissions) or the biomass burning emission sources implemented in the
 445 model. These categories include direct emissions of CO (for both anthropogenic and biomass burning sources) and its NMVOC precursor emissions, as well as direct emissions of nitric oxide (NO). In these three sensitivity runs – hereafter referred to as the non-biogenic, non-anthropogenic and non-biomass burning simulations – CH₄ concentrations are based on measurements from NOAA. The results of these GEOS-Chem sensitivity simulations are compared to the standard run (results shown
 450 in Fig. 2). All four runs cover the mid-2005 to mid-2013 time period, hence starting a few years

before our period under investigation. This allows us to establish a stable situation for the period 2008 (most of the long-lived precursors of CO are removed from the atmosphere between mid-2005 and 2008). Figure 8 shows the CO total columns simulated by the different runs of GEOS-Chem for the three sites. The results for Paris and Jungfraujoch are quite similar. At these two sites, the seasonal variability of the CO loadings is mainly driven by anthropogenic emissions. Indeed, by shutting off the anthropogenic emissions of CO and of its NMVOC precursors, the amplitude of the CO seasonal variation and periodicity are radically reduced. This is in agreement with previous model studies. Duncan et al. (2007) show that fossil fuel emissions are the main contribution to the CO burden in the Northern extra-tropics. The high-altitude Jungfraujoch site is strongly impacted by long-range transport of CO. At least one third of it is of non-European origin (Duncan et al., 2007; Zellweger et al., 2009). Inversely, shutting off either biomass burning or biogenic emissions, only weakly affect the seasonal cycle and the maximum peaks. As compared to the standard run, CO columns are just a little bit lower due to some emissions missing. At Wollongong, the seasonal variability is mainly influenced by the biomass burning emissions: the highest peaks (e.g. at the end of 2009) disappear when the biomass burning component is removed from the simulation. The biogenic emissions provide the largest background contribution. Zeng et al. (2015) have observed that the impact of biogenic emissions on CO is larger in the Southern Hemisphere than in the Northern. Unlike at Paris and Jungfraujoch, the influence of anthropogenic emissions is negligible in the Wollongong simulation. We also note that the GEOS-Chem sensitivity runs provide the same results for the CO surface VMR, as for the CO total columns at the three studied sites.

5 Conclusions

This paper investigates the seasonal variability of CO total columns at three NDACC and/or TCCON sites: Paris and Jungfraujoch in the Northern Hemisphere and Wollongong in the Southern Hemisphere. In the Northern Hemisphere, the variability of CO above the PBL has a seasonal maximum in March-April and a minimum in September-October. In the Southern Hemisphere, this seasonal cycle is shifted by 6 months. We have compared the ground-based FTIR data to satellite measurements from IASI-MetOp and MOPITT and to GEOS-Chem model standard outputs, which confirm the observed CO seasonal variability. However with currently implemented inventories, an underestimation of about 20% by the GEOS-Chem model is observed, which is consistent with previous forward and inverse modelling studies. Interestingly, a time-lag of about 2 months between upper altitude and surface CO has been found in both Paris and Jungfraujoch. This time lag is likely linked to the different emission patterns. Custom simulations with emission sources being individually turned on and off show that the CO seasonality at Paris and Jungfraujoch is mainly controlled by anthropogenic emissions. In Wollongong, where low local anthropogenic emissions prevail and where the impact of biomass burning and biogenic emissions is large, such a time shift is neither observed nor

modelled. We have thus observed a temporal shift in the seasonal patterns at the surface and in the higher atmospheric layers for the sites that are strongly affected by local anthropogenic emissions. The observation of the time-lag is likely due to zonal mixing occurring on a shorter (1–2 weeks) timescale as complete vertical tropospheric mixing (1–2 months). In the future, it will be interesting
490 to study more closely the link between local and non-local emission sources and the magnitude of the time shift between surface and total column CO by extending the present study on more sites and to improve the analysis of the temporal signals. The presence of global ground-based FTIR networks provides a unique opportunity to obtain these data on a global scale, as the instruments are capable of studying the surface and the total column data at the same time. The time lag data might also
495 provide an additional benchmark parameter for chemical transport models and emission inventories, taking into account that the modeling of vertical CO gradients in the remote Southern Hemisphere already provides a challenge for chemical transport modeling (Fisher et al., 2015).

Acknowledgements. We are grateful to Université Pierre et Marie Curie and Région Île-de-France for their financial contributions and to Institut Pierre-Simon Laplace for support and facilities. We thank the National
500 Center for Atmospheric Research MOPITT science team and NASA for producing and archiving the MOPITT CO product. Thanks are also due to the Swiss National Air Pollution Monitoring Network (NABEL) for delivering ground data around Switzerland. The University of Liège contribution to the present work has primarily been supported by the F.R.S. – FNRS, the Fédération Wallonie-Bruxelles and MeteoSwiss (GAW-CH program). We thank the International Foundation High Altitude Research Stations Jungfrauoch and Gornergrat (HFSJG,
505 Bern). We are grateful to all colleagues who contributed to the acquisition of the FTIR data. The NDACC datasets used here are publicly available from the network database (<ftp://ftp.cpc.ncep.noaa.gov/ndacc/station>). The Australian Research Council has provided financial support over the years for the NDACC site at Wollongong, most recently as part of project DP110101948. We also acknowledge the important contribution to the measurement program at Wollongong made by researchers other than those listed as co-authors here, including amongst others, Voltaire Velazco and Nicholas Deutscher. IASI has been developed and built under the
510 responsibility of the French space agency CNES. It is flown onboard the MetOp satellite as part of the Eumetsat Polar System (EPS). The IASI L1 data are received through the Eumetcast near real time data distribution service. IASI L1 and L2 data are stored in the French atmospheric database Ether (<http://ether.ipsl.jussieu.fr>). The National Center for Atmospheric Research (NCAR) is sponsored by the National Science Foundation. Any
515 opinions, findings and conclusions or recommendations expressed in the publication are those of the author(s) and do not necessarily reflect the views of the National Science Foundation.

[Table 1 about here.]

[Table 2 about here.]

References

- 520 August, T., Klaes, D., Schlüssel, P., Hultberg, T., Crapeau, M., Arriaga, A., O'Carroll, A., Coppens, D., Munro, R., and Calbet, X.: IASI on MetOp-A: Operational Level 2 retrievals after five years in orbit, *J. Quant. Spectroscop. Radiat. Transfer*, 113, 1340–1371, doi:10.1016/j.jqsrt.2012.02.028, 2012.
- Bakwin, P. S., Tans, P. P., and Novelli, P. C.: Carbon monoxide budget in the northern hemisphere, *Geophys. Res. Lett.*, 21, 433–436, 1994.
- 525 Barret, B., Mazière, D. M., and Mahieu, E.: Ground-based FTIR measurements of CO from the Jungfraujoeh: characterisation and comparison with in situ surface and MOPITT data, *Atmos. Chem. Phys.*, 3, 2217–2223, doi:10.5194/acp-3-2217-2003, 2003.
- Bekki, S., Law, K. S., and Pyle, J. A.: Effect of ozone depletion on atmospheric CH₄ and CO concentrations, *Nature*, 371, 595–597, doi:10.1038/371595a0, 1994.
- 530 Benedictow, A., Berge, H., Fagerli, H., Gauss, M., Jonson, J. E., Nyíri, A., Simpson, D., Tsyro, S., Valdebenito, A., Shamsudheen, V. S., Wind, P., Aas, W., Hjellbrekke, A.-G., Mareckova, K., Wankmüller, R., Iversen, T., Kirkevåg, A., Seland, Ø., Haugen, J. E., and Mills, G.: Transboundary acidification, eutrophication and ground level ozone in Europe in 2008, Tech. rep., The Norwegian Meteorological Institute, Oslo, Norway, 2010.
- 535 Bey, I., Jacob, D. J., Yantosca, R. M., Logan, J. A., Field, B. D., Fiore, A. M., Li, Q., Liu, H. Y., Mickley, L. J., and Schultz, M. G.: Global modeling of tropospheric chemistry with assimilated meteorology: model description and evaluation, *J. Geophys. Res.-Atmos.*, 106, 23 073–23 095, doi:10.1029/2001JD000807, 2001.
- Blumstein, D., Chalon, G., Carlier, T., Buil, C., Hebert, P., Maciaszek, T., Ponce, G., Phulpin, T., Tournier, B., Simeoni, D., Astruc, P., Clauss, A., Kayal, G., and Jegou, R.: IASI instrument: technical overview and measured performances, in: *Proc. SPIE 5543, Infrared Spaceborne Remote Sensing XII*, doi:10.1117/12.560907, 2004.
- 540 Bousquet, P., Hauglustaine, D. A., Peylin, P., Carouge, C., and Ciais, P.: Two decades of OH variability as inferred by an inversion of atmospheric transport and chemistry of methyl chloroform, *Atmos. Chem. Phys.*, 5, 2635–2656, doi:10.5194/acp-5-2635-2005, 2005.
- 545 Brunke, E.-G., Scheel, H., and Seiler, W.: Trends of tropospheric CO, N₂O and CH₄ as observed at cape point, South Africa, *Atmos. Environ.*, 24, 585–595, doi:10.1016/0960-1686(90)90013-D, 1990.
- Buchholz, R. R., Paton-Walsh, C., Griffith, D. W. T., Kubistin, D., Caldow, C., Fisher, J. A., Deutscher, N. M., Kettlewell, G., Riggensbach, M., Macatangay, R., Krummel, P. B., and Langenfelds, R. L.: Source and meteorological influences on air quality (CO, CH₄ & CO₂) at a Southern Hemisphere urban site, *Atmos. Environ.*, 126, 274–289, doi:10.1016/j.atmosenv.2015.11.041, 2016.
- 550 Clerbaux, C., George, M., Turquety, S., Walker, K. A., Barret, B., Bernath, P., Boone, C., Borsdorff, T., Cammas, J. P., Catoire, V., Coffey, M., Coheur, P.-F., Deeter, M., Mazière, D. M., Drummond, J., Duchatelet, P., Dupuy, E., Zafra, d. R., Eddounia, F., Edwards, D. P., Emmons, L., Funke, B., Gille, J., Griffith, D. W. T., Hannigan, J., Hase, F., Höpfner, M., Jones, N., Kagawa, A., Kasai, Y., Kramer, I., Flochmoën, L. E., Livesey, N. J., López-Puertas, M., Luo, M., Mahieu, E., Murtagh, D., Nédélec, P., Pazmino, A., Pumphrey, H., Ricaud, P., Rinsland, C. P., Robert, C., Schneider, M., Senten, C., Stiller, G., Strandberg, A., Strong, K., Sussmann, R., Thouret, V., Urban, J., and Wiacek, A.: CO measurements from the ACE-FTS satellite instrument: data

- analysis and validation using ground-based, airborne and spaceborne observations, *Atmos. Chem. Phys.*, 8, 2569–2594, doi:10.5194/acp-8-2569-2008, 2008.
- 560 Clerbaux, C., Boynard, A., Clarisse, L., George, M., Hadji-Lazaro, J., Herbin, H., Hurtmans, D., Pommier, M., Razavi, A., Turquety, S., Wespes, C., and Coheur, P.-F.: Monitoring of atmospheric composition using the thermal infrared IASI/MetOp sounder, *Atmos. Chem. Phys.*, 9, 6041–6054, doi:10.5194/acp-9-6041-2009, 2009.
- Deeter, M., Emmons, L., Francis, G., Edwards, D., Gille, J., Warner, J., Khattatov, B., Ziskin, D., Lamarque, J.-F., Ho, S.-P., Yudin, V., Attié, J.-L., Packman, D., Chen, J., Mao, D., Drummond, J., Novelli, P., and Sachse, G.: Evaluation of operational radiances for the Measurements of Pollution in the Troposphere (MOPITT) instrument CO thermal band channels, *J. Geophys. Res.*, 109, D03 308, doi:10.1029/2003JD003970, 2004.
- 565 Dils, B., Cui, J., Henne, S., Mahieu, E., Steinbacher, M., and Mazière, D. M.: CO trend at the high Alpine site Jungfraujoch: a comparison between NDIR surface in situ and FTIR remote sensing observations, *Atmos. Chem. Phys.*, 11, 6735–6748, doi:10.5194/acp-11-6735-2011, 2011.
- Drummond, J. and Mand, G.: The Measurements of Pollution in the Troposphere (MOPITT) Instrument: Overall Performance and Calibration Requirements, *J. Atmos. Ocean. Technol.*, 13, 314, 1996.
- Duchatelet, P., Demoulin, P., Hase, F., Ruhnke, R., Feng, W., Chipperfield, M. P., Bernath, P. F., Boone, C. D., Walker, K. A., and Mahieu, E.: Hydrogen fluoride (HF) total and partial column time series above the Jungfraujoch from long-term FTIR measurements: impact of the line-shape model, error budget, seasonal cycle and comparison with satellite and model data, *J. Geophys. Res.*, 115, D22 306, doi:10.1029/2010JD014677, 2010.
- 570 Duncan, B. N., Logan, J. A., Bey, I., Megretskaia, I. A., Yantosca, R. M., Novelli, P. C. Jones, N. B., and Rinsland, C. P.: Global budget of CO, 1988–1997: Source estimates and validation with a global model, *J. Geophys. Res. Atmos.*, 112, doi:10.1029/2007JD008459, d22301, 2007.
- Edwards, D. P., Pétron, G., Novelli, P. C., Emmons, L. K., Gille, J. C., and Drummond, J. R.: Southern Hemisphere carbon monoxide interannual variability observed by Terra/Measurement of Pollution in the Troposphere (MOPITT), *J. Geophys. Res.*, 111, D16 303, doi:10.1029/2006JD007079, 2006.
- Esposito, F., Grieco, G., Masiello, G., Pavese, G., Restieri, R., Serio, C., and Cuomo, V.: Intercomparison of line-parameter spectroscopic databases using downwelling spectral radiance, *Quart. J. Roy. Met. Soc.*, 133, 191–202, doi:10.1002/qj.131, 2007.
- 585 Fisher, J. A., Wilson, S. R., Zeng, G., Williams, J. E., Emmons, L. K., Langenfelds, R. L., Krummel, P. B., and Steele, L. P.: Seasonal changes in the tropospheric carbon monoxide profile over the remote Southern Hemisphere evaluated using multi-model simulations and aircraft observations, *Atmos. Chem. Phys.*, 15, 3217–3239, doi:10.5194/acp-15-3217-2015, 2015.
- George, M., Clerbaux, C., Hurtmans, D., Turquety, S., Coheur, P.-F., Pommier, M., Hadji-Lazaro, J., Edwards, D. P., Worden, H., Luo, M., Rinsland, C., and McMillan, W.: Carbon monoxide distributions from the IASI/METOP mission: evaluation with other space-borne remote sensors, *Atmos. Chem. Phys.*, 9, 8317–8330, doi:10.5194/acp-9-8317-2009, 2009.
- 595 Griffith, D. W. T.: Synthetic Calibration and Quantitative Analysis of Gas-Phase infrared Spectra, *Appl. Spectroscop.*, 50, 59–70, 1996.

- Griffith, D. W. T., Deutscher, N. M., Caldow, C. G. R., Kettlewell, G., Riggenbach, M., and Hammer, S.: A Fourier transform infrared trace gas and isotope analyser for atmospheric applications, *Atmos. Meas. Tech.*, 5, 2012.
- 600 Guenther, A., Karl, T., Harley, P., Wiedinmyer, C., Palmer, P. I., and Geron, C.: Estimates of global terrestrial isoprene emissions using MEGAN (Model of Emissions of Gases and Aerosols from Nature), *Atmos. Chem. Phys.*, 6, 10–5194, 2006.
- Hase, F., Hannigan, J. W., Coey, M. T., Goldman, A., Höpfner, M., Jones, N. B., Rinsland, C. P., and Wood, S. W.: Intercomparison of retrieval codes used for the analysis of high-resolution: ground-based FTIR measurements, *J. Quant. Spectroscop. Radiat. Transfer*, 87, 25–52, 2004.
- 605 Hase, F., Demoulin, P., Sauval, A. J., Toon, G. C., Bernath, P. F., Goldman, A., Hannigan, J. W., and Rinsland, C. P.: An empirical line-by-line model for the infrared solar transmittance spectrum from 700 to 5000 cm^{-1} , *J. Quant. Spectroscop. Radiat. Transfer*, 102, 450–463, doi:10.1016/j.jqsrt.2006.02.026, 2006.
- Holloway, T., Levy, H., and Kasibhatla, P.: Global distribution of carbon monoxide, *J. Geophys. Res. Atmos.*, 610 105, 12 123–12 147, doi:10.1029/1999JD901173, 2000.
- Hooghiemstra, P. B., Krol, M. C., Bergamaschi, P., de Laat, A. T. J., van der Werf, G. R., Novelli, P. C., Deeter, M. N., Aben, I., and Röckmann, T.: Comparing optimized CO emission estimates using MOPITT or NOAA surface network observations, *J. Geophys. Res.*, 117, D06 309–23, 2012.
- Hurtmans, D., Coheur, P.-F., Wespes, C., Clarisse, L., Scharf, O., Clerbaux, C., Hadji-Lazaro, J., George, M., and Turquety, S.: FORLI radiative transfer and retrieval code for IASI, *J. Quant. Spectroscop. Radiat. Transfer*, 113, 1391–1408, doi:10.1016/j.jqsrt.2012.02.036, 2006.
- 615 Khalil, M. A. K. and Rasmussen, R. A.: Carbon monoxide in the Earth’s atmosphere: indications of a global increase, *Nature*, 332, 242–245, doi:10.1038/332242a0, 1988.
- Khalil, M. A. K. and Rasmussen, R. A.: Global decrease in atmospheric carbon monoxide concentration, *Nature*, 620 370, 639–641, doi:10.1038/370639a0, 1994.
- Kopacz, M., Jacob, D. J., Fisher, J. A., Logan, J. A., Zhang, L., Megretskaja, I. A., Yantosca, R. M., Singh, K., Henze, D. K., Burrows, J. P., Buchwitz, M., Khlystova, I., McMillan, W. W., Gille, J. C., Edwards, D. P., Eldering, A., Thouret, V., and Nedelec, P.: Global estimates of CO sources with high resolution by adjoint inversion of multiple satellite datasets (MOPITT, AIRS, SCIAMACHY, TES), *Atmos. Chem. Phys.*, 10, 855–876, 2010.
- 625 Logan, J. A., Prather, M. J., Wofsy, F. C., and McElroy, M. B.: Tropospheric Chemistry: A Global Perspective, *J. Geophys. Res.*, 86, 7210–7254, 1981.
- Mahieu, E., Zander, R., Delbouille, L., Demoulin, P., Roland, G., and Servais, C.: Observed Trends in Total Vertical Column Abundances of Atmospheric Gases from IR Solar Spectra Recorded at the Jungfraujoch, *J. Atmos. Chem.*, 28, 227–243, doi:10.1023/A:1005854926740, 1997.
- 630 Mao, J., Jacob, D. J., Evans, M. J., Olson, J. R., Ren, X., Brune, W. H., Clair, S. J. M., Crounse, J. D., Spencer, K. M., Beaver, M. R., Wennberg, P. O., Cubison, M. J., Jimenez, J. L., Fried, A., Weibring, P., Walega, J. G., Hall, S. R., Weinheimer, A. J., Cohen, R. C., Chen, G., Crawford, J. H., McNaughton, C., Clarke, A. D., Jaeglé, L., Fisher, J. A., Yantosca, R. M., Sager, L. P., and Carouge, C.: Chemistry of hydrogen oxide radicals (HOx) in the Arctic troposphere in spring, *Atmos. Chem. Phys.*, 10, 5823–5838, doi:10.5194/acp-10-5823-2010, 2010.
- 635

- Novelli, P. C., Masarie, K. A., Tans, P. P., and Lang, P. M.: Recent Changes in Atmospheric Carbon Monoxide, *Science*, 263, 1587–1590, doi:10.1126/science.263.5153.1587, 1994.
- Novelli, P. C., Masarie, K. A., and Lang, P. M.: Distributions and recent changes of carbon monoxide in the
640 lower troposphere, *J. Geophys. Res. Atmos.*, 103, 19 015–19 033, doi:10.1029/98JD01366, 1998.
- Novelli, P. C., Masarie, K. A., Lang, P. M., Hall, B. D., Myers, R. C., and Elkins, J. W.: Reanalysis of tropospheric CO trends: Effects of the 1997–1998 wildfires, *J. Geophys. Res. Atmos.*, 108, doi:10.1029/2002JD003031, 4464, 2003.
- Olivier, J. G. J. and Berdowski, J. J. M.: Global emissions sources and sinks., in: *The Climate System*, edited
645 by Berdowski, J., Guicherit, R., and Heij, B., pp. 33–78, A.A. Balkema Publishers/Swets & Zeitlinger Publishers, Lisse, The Netherlands, 2001.
- Park, R. J., Jacob, D. J., Field, B. D., Yantosca, R. M., and Chin, M.: Natural and transboundary pollution influences on sulfate-nitrate-ammonium aerosols in the United States: implications for policy, *J. Geophys. Res.*, 109, D15 204, doi:10.1029/2003JD004473, 2004.
- 650 Pougatchev, N. S. and Rinsland, C. P.: Spectroscopic study of the seasonal variation of carbon monoxide vertical distribution above Kitt Peak, *J. Geophys. Res.*, 100, 1409–1416, 1995.
- Rinsland, C. P., Jones, N. B., Connor, B. J., Logan, J. A., Pougatchev, N. S., Goldman, A., Murcray, F. J., Stephen, T. M., Pine, A. S., Zander, R., Mahieu, E., and Demoulin, P.: Northern and southern hemisphere ground-based infrared spectroscopic measurements of tropospheric carbon monoxide and ethane, *J. Geophys. Res.*, 103, 28 197, doi:10.1029/98JD02515, 1998.
- 655 Rinsland, C. P., Goldman, A., Murcray, F. J., Stephen, T. M., Pougatchev, N. S., Fishman, J., David, S. J., Blatherwick, R. D., Novelli, P. C., Jones, N. B., and Connor, B. J.: Infrared solar spectroscopic measurements of free tropospheric CO, C₂H₆, and HCN above Mauna Loa, Hawaii: Seasonal variations and evidence for enhanced emissions from the Southeast Asian tropical fires of 1997–1998, *J. Geophys. Res. Atmos.*, 104, 18 667–18 680, doi:10.1029/1999JD900366, 1999.
- 660 Rinsland, C. P., Mahieu, E., Zander, R., Demoulin, P., Forrer, J., and Buchmann, B.: Free tropospheric CO, C₂H₆, and HCN above central Europe: Recent measurements from the Jungfraujoch station including the detection of elevated columns during 1998, *J. Geophys. Res.*, 105, 24 235–24 249, 2000.
- Rinsland, C. P., Meier, A., Griffith, D. W. T., and Chiou, L. S.: Ground-based measurements of tropospheric
665 CO, C₂H₆, and HCN from Australia at 34°S latitude during 1997–1998, *J. Geophys. Res. Atmos.*, 106, 20 913–20 924, doi:10.1029/2000JD000318, 2001.
- Rinsland, C. P., Goldman, A., Hannigan, J. W., Wood, S. W., Chiou, L. S., and Mahieu, E.: Long-term trends of tropospheric carbon monoxide and hydrogen cyanide from analysis of high resolution infrared solar spectra, *J. Quant. Spectroscop. Radiat. Transfer*, 104, 40–51, 2007.
- 670 Rodgers, C. D.: Characterization and error analysis of profiles retrieved from remote sounding measurements, *J. Geophys. Res.*, 95, doi:10.1029/JD095iD05p05587, 1990.
- Rodgers, C. D. and Connor, B. J.: Intercomparison of remote sounding instruments, *J. Geophys. Res.*, 108, 4116–4129, doi:10.1029/2002JD002299, 2003.
- Rohrer, F. and Berresheim, H.: Strong correlation between levels of tropospheric hydroxyl radicals and solar
675 ultraviolet radiation, *Nature*, 442, 184–187, doi:10.1038/nature04924, 2006.

- Rothman, L. S., Jacquemart, D., Barbe, A., Benner, D. C., Birk, M., Brown, L. R., Carleer, M. R., Chackerian, Jr. C., Chance, K., Coudert, L. H., Dana, V., Devi, V. M., Flaud, J.-M., Gamache, R. R., Goldman, A., Hartmann, J.-M., Jucks, K. W., Maki, A. G., Mandin, J.-Y., Massie, S. T., Orphal, J., Perrin, A., Rinsland, C. P., Smith, M. A. H., Tennyson, J., Tolchenov, R. N., Toth, R. A., Vander Auwera, J., Varanasi, P., and Wagner, G.: The HITRAN 2004 Molecular Spectroscopic Database, *J. Quant. Spectrosc. Radiat. Trans.*, 96, 139 – 204, 2005.
- 680 Rothman, L. S., Gordon, I. E., Barbe, A., Benner, D. C., Bernath, P. F., Birk, M., Boudon, V., Brown, L. R., Campargue, A., Champion, J. P., Chance, K., Coudert, L. H., Dana, V., Devi, V. M., Fally, S., Flaud, J. M., Gamache, R. R., Goldman, A., Jacquemart, D., Kleiner, I., Lacome, N., Lafferty, W. J., Mandin, J. Y., Massie, S. T., Mikhailenko, S. N., Miller, C. E., Moazzen-Ahmadi, N., Naumenko, O. V., Nikitin, A. V., Orphal, J., Perevalov, V. I., Perrin, A., Predoi-Cross, A., Rinsland, C. P., Rotger, M., Simecková, M., Smith, M. A. H., Sung, K., Tashkun, S. A., Tennyson, J., Toth, R. A., Vandaele, A. C., and Vander Auwera, J.: The HITRAN 2008 molecular spectroscopic database, *J. Quant. Spectrosc. Radiat. Trans.*, 110, 533–572, 2009.
- 685 Schneider, M., Yoshimura, K., Hase, F., and Blumenstock, T.: The ground-based FTIR network's potential for investigating the atmospheric water cycle, *Atmos. Chem. Phys.*, 10, 3427–3442, 2010.
- 690 Schultz, M., Backman, L., Balkanski, Y., Bjoernsdalsaeter, S., Brand, R., Burrows, J., Dalsoeren, S., de Vasconcelos, M., Grodtmann, B., Hauglustaine, D., Heil, A., Hoelzemann, J., Isaksen, I., Kaurola, J., Knorr, W., Ladstaetter-Weissenmayer, A., Mota, B., Oom, D., Pacyna, J., Panasiuk, D., Pereira, J., Pulles, T., Pyle, J., Rast, S., Richter, A., Savage, N., Schnadt, C., Schulz, M., Spessa, A., Staehelin, J., Sundet, J., Szopa, S., Thonicke, K., van het Bolscher, M., van Noije, T., van Velthoven, P., Vik, A., and Wittrock, F.: REanalysis of the TROpospheric chemical composition over the past 40 years – A long-term global modeling study of tropospheric chemistry, final report 48/2007, Max Planck Institute for Meteorology, Hamburg, Germany, 2007.
- 700 Street, J. O., Carroll, R. J., and Ruppert, D.: A Note on Computing Robust Regression Estimates via Iteratively Reweighted Least Squares, *Am. Stat.*, 42, 152–154, doi:10.1080/00031305.1988.10475548, 1988.
- Té, Y., Jeseck, P., Payan, S., Pépin, I., and Camy-Peyret, C.: The Fourier transform spectrometer of the UPMC University QualAir platform, *Rev. Sci. Instrum.*, 81, 103 102–10, doi:10.1063/1.3488357, 2010.
- 705 Té, Y., Dieudonné, E., Jeseck, P., Hase, F., Hadji-Lazaro, J., Clerbaux, C., Ravetta, F., Payan, S., Pépin, I., Hurtmans, D., Pelon, J., and Camy-Peyret, C.: Carbon monoxide urban emission monitoring: a ground-based FTIR case study, *J. Atmos. Oceanic Technol.*, 29, 911–921, doi:10.1175/JTECH-D-11-00040.1, 2012.
- Thompson, A. M.: The oxidizing capacity of the earth's atmosphere: Probable past and future changes, *Science*, 286, 1157–1165, doi:10.1126/science.256.5060.1157, 1992.
- 710 Thompson, A. M., Huntley, M. A., and Stewart, R. W.: Perturbations to tropospheric oxidants, 1985–2035: 1. Calculations of ozone and OH in chemically coherent regions, *J. Geophys. Res.*, 95, 9829–9844, doi:10.1029/JD095iD07p09829, 1990.
- Tournier, B., Blumstein, D., Cayla, F.-R., and Chalon, G.: IASI level 0 and 1 processing algorithms description, in: *Proc. 12th Int. TOVS Study Conf. (ITSC-XII)*, Lorne, VIC, Australia, 2002.
- van der Werf, G. R., Randerson, J. T., Giglio, L., Collatz, G. J., Mu, M., Kasibhatla, P. S., Morton, D. C., DeFries, R. S., Jin, Y., and Leeuwen, v. T. T.: Global fire emissions and the contribution of deforestation,

- 715 savanna, forest, agricultural, and peat fires, *Atmos. Chem. Phys.*, 10, 11 707–11 735, doi:10.5194/acp-10-11707-2010, 2010.
- van Donkelaar, A., Martin, R. V., Leaitch, W. R., MacDonald, A. M., Walker, T. W., Streets, D. G., Zhang, Q., Dunlea, E. J., Jimenez, J. L., Dibb, J. E., Huey, L. G., Weber, R., and Andreae, M. O.: Analysis of aircraft and satellite measurements from the Intercontinental Chemical Transport Experiment (INTEX-B) to quantify long-range transport of East Asian sulfur to Canada, *Atmos. Chem. Phys.*, 8, 10–5194, doi:10.5194/acp-8-2999-2008, 2008.
- 720
- Viatte, C., Schneider, M., Redondas, A., Hase, F., Eremenko, M., Chelin, P., Flaud, J.-M., Blumenstock, T., and Orphal, J.: Comparison of ground-based FTIR and Brewer O₃ total column with data from two different IASI algorithms and from OMI and GOME-2 satellite instruments, *Atmos. Meas. Tech.*, 4, 535–546, doi:10.5194/amt-4-535-2011, 2011.
- 725
- Weinstock, B.: Carbon Monoxide: Residence Time in the Atmosphere, *Science*, 166, 224–225, 1969.
- Worden, H. M., Deeter, M. N., Edwards, D. P., Gille, J. C., Drummond, J. R., and Nédélec, P.: Observations of near-surface carbon monoxide from space using MOPITT multispectral retrievals, *J. Geophys. Res. Atmos.*, 115, doi:10.1029/2010JD014242, d18314, 2010.
- 730
- Xiao, Y., Logan, J. A., Jacob, D. J., Hudman, R. C., Yantosca, R., and Blake, D. R.: Global budget of ethane and regional constraints on U.S. sources, *J. Geophys. Res.*, 113, 21 306–10, doi:10.1029/2007JD009415, 2008.
- Yurganov, L. N., Blumenstock, T., Grechko, E. I., Hase, F., Hyer, E. J., Kasischke, E. S., Koike, M., Kondo, Y., Kramer, I., Leung, F.-Y., Mahieu, E., Mellqvist, J., Notholt, J., Novelli, P. C., Rinsland, C. P., Scheel, H. E., Schulz, A., Strandberg, A., Sussmann, R., Tanimoto, H., Velazco, V., Zander, R., and Zhao, Y.: A quantitative assessment of the 1998 carbon monoxide emission anomaly in the Northern Hemisphere based on total column and surface concentration measurements, *J. Geophys. Res. Atmos.*, 109, doi:10.1029/2004JD004559, d15305, 2004.
- 735
- Yurganov, L. N., Duchatelet, P., Dzhola, A. V., Edwards, D. P., Hase, F., Kramer, I., Mahieu, E., Mellqvist, J., Notholt, J., Novelli, P. C., Rockmann, A., Scheel, H. E., Schneider, M., Schulz, A., Strandberg, A., Sussmann, R., Tanimoto, H., Velazco, V., Drummond, J. R., and Gille, J. C.: Increased Northern Hemispheric carbon monoxide burden in the troposphere in 2002 and 2003 detected from the ground and from space, *Atmos. Chem. and Phys.*, 5, 563–573, doi:10.5194/acp-5-563-2005, 2005.
- 740
- Zander, R., Demoulin, P., Ehhalt, D. H., Schmidt, U., and Rinsland, C. P.: Secular increase of the total vertical column abundance of carbon monoxide above central Europe since 1950, *J. Geophys. Res. Atmos.*, 94, 11 021–11 028, doi:10.1029/JD094iD08p11021, 1989.
- 745
- Zander, R., Mahieu, E., Demoulin, P., Duchatelet, P., Roland, G., Servais, C., Mazière, D. M., Reimann, S., and Rinsland, C. P.: Our changing atmosphere: Evidence based on long-term infrared solar observations at the Jungfraujoch since 1950, *Sci. Tot. Environ.*, 391, 184–195, doi:10.1016/j.scitotenv.2007.10.018, 2008.
- Zbinden, R. M., Thouret, V., Ricaud, P., Carminati, F., Cammas, J.-P., and Nédélec, P.: Climatology of pure tropospheric profiles and column contents of ozone and carbon monoxide using MOZAIC, *Atmos. Chem. Phys.*, 13, 12 363–12 388, doi:10.5194/acp-13-12363-2013, 2013.
- 750
- Zellweger, C., Hüglin, C., Klausen, J., Steinbacher, M., Vollmer, M., and Buchmann, B.: Inter-comparison of four different carbon monoxide measurement techniques and evaluation of the long-term carbon monoxide time series of Jungfraujoch, *Atmos. Chem. Phys.*, 9, 3491–3503, doi:10.5194/acp-9-3491-2009, 2009.

- 755 Zeng, G., Williams, J. E., Fisher, J. A., Emmons, L. K., Jones, N. B., Morgenstern, O., Robinson, J., Smale, D., Paton-Walsh, C., and Griffith, D. W. T.: Multi-model simulation of CO and HCHO in the Southern Hemisphere: comparison with observations and impact of biogenic emissions, *Atmos. Chem. Phys.*, 15, 7217–7245, 2015.
- 760 Zhao, Y., Kondo, Y., Murcray, F. J., Liu, X., Koike, M., Kita, K., Nakajima, H., Murata, I., and Suzuki, K.: Carbon monoxide column abundances and tropospheric concentrations retrieved from high resolution ground-based infrared solar spectra at 43.5°N over Japan, *J. Geophys. Res.*, 102, 23 403–23 411, 1997.
- Zhao, Y., Strong, K., Kondo, Y., Koike, M., Matsumi, Y., Irie, Y., Rinsland, H., C, P., Jones, N. B., Suzuki, K., Nakajima, H., Nakane, H., and Murata, I.: Spectroscopic measurements of tropospheric CO, C₂H₆, C₂H₂ and HCN in Northern Japan, *J. Geophys. Res.*, 107, 4343, doi:10.1029/2001JD000748, 2002.

Table 1. Ground-based FTIR instrumental information and details concerning the configuration used to record the measurements at the three studied sites

	Paris	Jungfraujoch	Wollongong
Sun-tracker model	A547 (Bruker Optics)	Home made	A547 (Bruker Optics)
Sun-tracker accuracy	< 1 arcmin	< 6 arcmin	< 1 arcmin
Spectrometer	IFS 125HR	IFS 120HR	IFS 125HR
Network	TCCON with NDACC measurements	NDACC	NDACC and TCCON
Optical Path Difference	257 cm	114 to 175 cm	257 cm
Integration time	205 s	135 to 1035 s	206 s
	(2 co-additions)	(depending on co-addition and OPD)	(2 co-additions)
Entrance window	CaF ₂ (instrument under vacuum)	None (instrument not under vacuum)	KBr (instrument under vacuum)
Beamsplitter	CaF ₂	KBr	CaF ₂
Optical filter	Yes	Yes	Yes
Detector	InSb	InSb	InSb
Spectral range	3.8 to 5.1 μm	4.4 to 6 μm	4.4 to 5.1 μm

Table 2. Parameters obtained from the sinusoidal fit of the seasonal variability to the CO total columns from ground-based, satellite and GEOS-Chem modeling data

	Paris		Jungfraujoch		Wollongong	
	Half-period (w) (days)	Amplitude (A) (%)	Half-period (w) (days)	Amplitude (A) (%)	Half-period (w) (days)	Amplitude (A) (%)
Ground-based	191 ± 3	14 ± 1	185 ± 1	12 ± 1	178 ± 1	17 ± 1
Satellite data	183 ± 1	14 ± 1	190 ± 2	12 ± 1	182 ± 1	16 ± 1
GEOS-Chem	183 ± 1	19 ± 1	182 ± 1	12 ± 1	180 ± 1	13 ± 1